Spectroscopic and Theoretical Evidence for the Elusive Intermediate of the Photoinitiated and Thermal Rearrangements of Photochromic Spiropyrans

Vladimir I. Minkin,*,†,‡ Anatoly V. Metelitsa,† Igor V. Dorogan,† Boris S. Lukyanov,† Serguei O. Besugliy,†,‡ and Jean-Claude Micheau†,§

Institute of Physical and Organic Chemistry, Rostov University, Stachka Avenue 194/2, 344090, Rostov on Don, Russian Federation, Division of Physical Organic Chemistry, Southern Scientific Center of Russian Academy of Science, 41, Chekhov Street, 344006 Rostov on Don, Russian Federation, and Université P. Sabatier, UMR CNRS 5623, IMRCP, 118 Route de Narbonne, F-31062, Toulouse, France

Received: February 1, 2005; In Final Form: August 30, 2005

Spectral properties and photochromic behavior of a series of novel 1′,3′,3′-trimethyl-1,2-tetramethylenespiro-[7*H*-furo(3,2-*f*)-(2*H*-1)-benzopyran-7,2′-indolines] **1**−**4** have been studied. The mechanism of the photoinitiated ring-opening reaction involves the formation of an acoplanar cis−cisoid intermediate, the lifetime of which in the case of 6-(*tert*-butyl) derivative **4** is long enough to observe its absorption and fluorescence spectra under conditions of continuous irradiation. The occurrence of the intermediate on the reaction paths of the thermal and photochemical ring-opening processes has been also shown by the DFT and CIS calculations. The TD-B3LYP/6-31G**//HF/6-31G** calculated spectrum of the intermediate well matches that observed experimentally. For spiropyran **3** with a 6-NO_2 group, kinetic and activation parameters of the photoinitiated coloration and dark bleaching reactions have been determined.

1. Introduction

Spiropyrans are among the most amply studied families of photochromic compounds.[1] Exhibiting high quantum efficiency of their photoinitiated rearrangements governed by the reversible photochemical cleavage of the C_{spiro}−O bond in the 2*H*-chromene ring (Scheme 1, where **TTC** and **CTC** stand for, respectively, *s*-trans−trans−*s*-cis and *s*-cis−trans−*s*-cis forms of the colored merocyanine isomers) and possessing high two-photon absorption coefficients, the largest among the photochromic compounds, spiropyrans, have a significant potential for diverse technical applications such as molecular switches and high-density photochemical erasable memories.[2]

To enhance the above indicated important properties of spiropyrans and to amend the principal drawbacks of this class of photochromic compounds caused by generally low-energy barriers to their dark back ring-closing reactions and insufficient fatigue resistance, extensive synthetic work on structural modifications of spiropyran molecules continues to be carried out. For a targeted approach to these goals, comprehension of the mechanisms of both photoinitiated and thermal reactions of the photochromic system is necessary, and considerable efforts have been devoted to gaining insight into the nature of the active states and intermediates of the reversible rearrangements of spiropyrans; see ref 3 for a recent review. The initial step of the photochromic reaction of spiropyrans is the dissociation of a C−O bond in an electronic excited state. The nature of the active excited state is determined by substitution in the benzopyran ring. Studies of the reaction dynamics with the use of time-resolved resonance Raman spectroscopy,[4] laser flash photolysis,[5] and quenching experiments[6] have shown that, for spiropyrans with a nitro group, a triplet state plays a crucial role in the photochemical ring-opening reaction. The participation of the low-energy triplet state structures in the reaction hastens the photodegradation processes,[6,7] but they may be substantially dampened in the compounds having no substituents with low-lying π^*- and/or n-orbitals. For such spiropyrans, the mechanism of the photochemical reaction is represented by Scheme 2,[8] where the structure of the singlet excited state intermediate ^{1}**Sp*$_{perp}$** corresponds to that formed upon immediate cleavage of the C_{spiro}−O bond. According to the complete active space self-consistent field (CASSCF) modeling of this process,[9] the structure similar to ^{1}**Sp*$_{perp}$** in Scheme 2 does not conform to a real intermediate but to a crossing point, i.e., a conical intersection between the lowest singlet excited and ground state energy surfaces. At this point, two reaction valleys are generated, one of which leads to ring closing to the initial spirocyclic form and another one to the formation of the *s*-cis−cis−*s*-cis (**CCC**) ring-opened form. The existence of this intermediate, usually designated the **X**-form, was first proposed[10] in the study of the photochemistry of spiropyrans in low-temperature matrixes. On the basis of nano-, pico-, and femtosecond spectroscopic data,[11] the acoplanar cis−cisoid structures (**CCC**) corresponding to **X** in Scheme 1 were assigned to the primary photoproducts that emerge after excitation at the longest wavelength of the ring-closed form of spiropyrans. In the case of 1′,3′,3′-trimethyl-6′-hydroxy-(2*H*-1)-benzopyran-2,2′-indoline, a part of a metastable species **X**,[11c] appearing in less than 100 fs after excitation at 300 nm, reestablishes the broken C_{spiro}−O bond on the time scale of 200 fs, whereas the rest converts to a mixture of merocyanine conformers with a decay time constant of about 100 ps. Similar mechanisms were also found to govern the photochromic behavior of spirooxazines,[3,12] which are the closest structural analogues of spiropyrans.

Although the time-resolved spectral studies bear rather convincing witness to the involvement of the acoplanar inter-

* Corresponding author. Telephone: +7 863 2434700. Fax: +7 863 2434667. E-mail: minkin@ipoc.rsu.ru.
† Rostov University.
‡ Southern Scientific Center of Russian Academy of Science.
§ Université P. Sabatier.

10.1021/jp050552+ CCC: $30.25
Published on Web 10/04/2005

SCHEME 1: General Scheme for the Reversible Rearrangement of Photochromic Spiropyrans

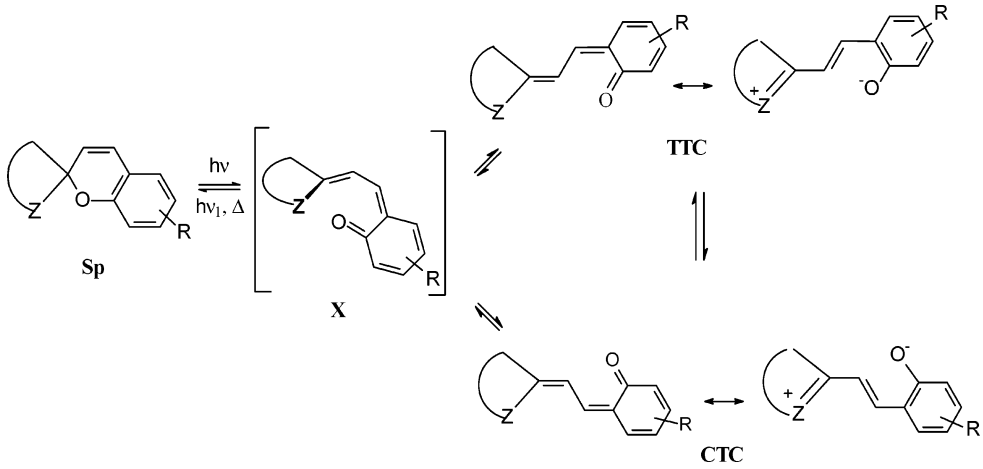

SCHEME 2: Principal Mechanism of the Photorearrangement of Spiropyrans in the Singlet Manifold

$$\mathbf{Sp} \xrightarrow{h\nu} {}^1\mathbf{Sp}^* \longrightarrow {}^1\mathbf{Sp}^*_{\mathbf{perp}}\mathbf{(X)} \longrightarrow \mathbf{CTC + TTC}$$

mediates **X** in the mechanism of the photochromic transformations shown in Scheme 1, there exists also an alternative interpretation of some of their results. Thus, it was pointed out[9] that the 100 and 200 fs processes observed in indolinobenzospiropyran transient absorption spectra may be attributed not to the formation and structural relaxation of the **CCC** intermediate, but to redistribution of the kinetic energy among the vibrational modes providing for stretching the $C_{spiro}-O$ bond and the subsequent decay through the conical intersection channel. It has been also argued that the peak around 490 nm observed in the femtosecond resolved transient absorption spectrum of 3′,3′-dimethyl-1′-methylspiro[2*H*-naphtho(1,2-*e*)-1,4-oxazine-2,2′-indoline] belongs not to the corresponding **CCC** intermediate, but is caused by the $S_n \leftarrow S_1$ absorption of the unbroken oxazine chromophore.[13] No **CCC**-type intermediate has yet been detected under standard conditions of continuous irradiation of solution of a spiropyran. One may expect that it would be possible to prolong the lifetime of the acoplanar isomer **X**, i.e., increase the energy barrier to its conversion to the energy-favored **CTC** and **TTC** forms, by stabilizing the former relative to the latter (destabilizing the latter relative to the former) in the spiropyrans with sterically strained merocyanine forms. In the simplest way, it may be realized in the spiropyrans containing bulky groups in positions 3 and 8 of a 2*H*-chromene ring. To examine this supposition, we have synthesized a series of spiro[7*H*-furo(3,2-*f*)-(2*H*-1)-benzopyran-7,2′-indolines] **1**−**4** shown in Scheme 3 and studied their photochromic behavior and spectral properties. Whereas several thousand diversely functionalized spiropyrans have been currently known and their photochromic properties reported, the compounds with a heterocyclic fragment in the photoresponsive 2*H*-chromene ring, known to possess enhanced persistence to photodegradation,[3] are rare in number and their study presents an independent interest.

2. Experimental Section

2.1. Synthesis. Spiropyrans **1**−**4** have been prepared following the previously described general procedures[14,15] in yields of 60−85%. **1**:[14] yellowish crystals, mp 164−165 °C. **2**: yellowish needles, mp 158−160 °C. **3**: dark-yellow needles, mp 139−140 °C. **4**: yellowish needles, mp 132−133 °C. The structures of compounds **1**, **2**, and **3** have been proved by X-ray determininations.[16]

2.2. Spectral Measurements. Absorption spectra were recorded on a thermostated Varian Cary 50 spectrometer. Solvents were of spectroscopic grade (Acros Organics). Low-temperature absorption spectra were recorded on a Specord UV−vis spectrophotometer equipped with a homemade apparatus allowing variation of the temperature of a solution between 77 and 293 K. Irradiation light was derived at 90° from

SCHEME 3: Structural Transformations of the Photochromic Spiropyrans 1−4

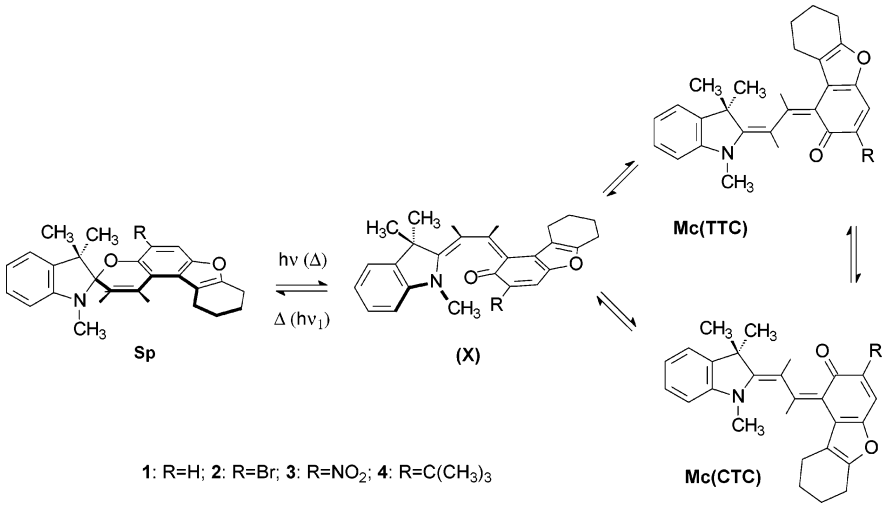

a 250 W high-pressure mercury lamp equipped with glass filters for allocation of lines of a mercury spectrum. The intensity of monochromatic light was determined using potassium ferrioxalate actinometry.

The luminescent measurements were carried out with Shimadzu RF-5001PC and Elumin 2M spectrofluorimeters. The fluorescence quantum yields were determined using 3-methoxybenzanthrone (quantum yield of fluorescence is 0.1, toluene) as a reference.

2.3. Kinetic Measurements. Photochromic parameters have been determined using photokinetic analysis of absorbance vs time curves recorded under continuous monochromatic irradiation[17,18] using an already described experimental setup.[19] To determine the desired parameters (Φ_1, Φ_2, $\epsilon_{Mc}(\lambda)$, $k_1(T)$, and $k_2(T)$), a differential equation (1) and a phenomenological equation (2) have been used:

$$-\mathrm{d}[\mathbf{Sp}]/\mathrm{d}t = I'_0F(\Phi_1\epsilon'_{Sp}[\mathbf{Sp}] - \Phi_2\epsilon'_{Mc}[\mathbf{Mc}]) + k_1[\mathbf{Sp}] - k_2[\mathbf{Mc}] \quad (1)$$

$$\mathrm{Abs}(\lambda) = \epsilon_{Sp}(\lambda)[\mathbf{Sp}] + \epsilon_{Mc}(\lambda)([\mathrm{C}]_0 - [\mathbf{Sp}]) \quad (2)$$

where $[C]_0$ is the initial concentration of the photochromic compound, $[C]_0 = [\mathbf{Sp}] + [\mathbf{Mc}]$; $\epsilon_{Sp}(\lambda)$ and $\epsilon_{Mc}(\lambda)$ ($l = 1$ cm) are the molar absorption coefficients of the **Sp** and **Mc** forms at wavelength λ. ϵ'_{Sp} and ϵ'_{Mc} values were taken at the irradiation wavelength (λ'). $F = (1 - 10^{-Abs'})/Abs'$ is the photokinetic factor;[20] I'_0 is the incident monochromatic photon flux. Φ_1 and Φ_2 are the quantum yields of photoreactions **Sp** → **Mc** and **Mc** → **Sp**; they are assumed to be wavelength independent. k_1 and k_2 are the thermal rate constants of the corresponding **Sp** → **Mc** and **Mc** → **Sp** dark processes. Experimental photokinetic curves (Abs_{exp} vs t) were fitted by the model (Abs_{calc}). The adjustable parameters are Φ_1, Φ_2, k_2, $\epsilon_{Sp}(313)$, $\epsilon_{Sp}(365)$, $\epsilon_{Mc}(313)$, $\epsilon_{Mc}(365)$, $\epsilon_{Mc}(546)$, $\epsilon_{Mc}(525)$, and $\epsilon_{Mc}(566)$. The robustness of the solution was demonstrated by showing that whatever their guessed initial values were, the same final set of parameters was delivered at convergence (Figure 1S, Supporting Information). The activation energies E_a's of **Sp** → **Mc** and **Mc** → **Sp** thermal reactions were calculated using the Arrhenius equation: $k(T) = k_0\exp(-E_a/RT)$. The thermodynamic parameters $\Delta H°$ and $\Delta S°$ were calculated from the dependence of equilibrium constants on temperature.

2.4. Computational Methods. Molecular geometries of the stationary points on the ground state potential energy surface (PES) of the isomers of spiropyran **4** were optimized using the B3LYP hybrid functional, which comprises the Becke[21] three-parameter exchange and Lee−Yang−Parr[22] correlation functionals with 3-21G** basis set. The nature of the stationary points on the PES was characterized by analyzing the Hessian force constant matrixes. Single point energy calculations of the structures were performed at the B3LYP/6-31G** level of approximation.

Calculations of the excitation energies were based on the TD-DFT method.[23] Since these values were found to be highly sensitive to the input molecular geometry, the structure corresponding to the intermediate **4(X)** on the ground state PES was reoptimized at the HF/6-31G** and B3LYP/6-31G** levels and subsequently used in TD-B3LYP/6-31G** calculations of spectral parameters. The configuration interaction with single excitations CIS/3-21G** method was employed to localize an intermediate of the ring-opening reaction of spiropyran **4** on the first singlet excited state PES.

Density functional theory (DFT) and ab initio calculations were carried out using the Gaussian 98[24] and GAMESS[25] sets of programs. For evaluating environmental effects on the geometry and electronic distribution of the merocyanine form of spiropyran **3**, semiempirical calculations based on the SM5.4/PM3[26a] solvation model as incorporated into the AMSOL 6.6[26b] program have been performed.

TABLE 1: Wavelengths of Maximum Absorption λ_{max} (in nm) and Corresponding Absorption Coefficients ϵ (in 10^3 L mol^{-1} cm^{-1}) in Parentheses of the Cyclic Forms of Spiropyrans 1 in Toluene and Ethanol Solutions at 293 K

	λ_{max} (ϵ)	
compound	toluene	ethanol
1	304 (18.2); 352[a] (3.2)	250 (21.2); 299 (21.8); 346[a] (3.2)
2	305 (21.0); 355[a] (5.1)	247 (24.5); 302 (21.4); 351[a] (4.8)
3	301 (19.2); 380[a] (5.1)	242 (19.60); 298 (18.0); 378[a] (5.8)
4	312 (13.9); 380 (9.0)	240 (30.6); 316 (15.8); 378 (10.9)

[a] A shoulder.

3. Results and Discussion

3.1. Absorption Spectra. In toluene solutions, all spiropyrans **1**−**4** exist as their ring-closed spiro forms (**Sp**). The longest wavelength absorption of compounds **1**−**3(Sp)** consists of a band with the maximum in the spectral region of 301−305 nm having a shoulder at 352−380 nm. For **4(Sp)**, the longest wavelength absorption band appears at 380 nm. Ethanol and acetonitrile solutions of spiropyrans **1**, **2**, and **4** are very weakly colored, which fact is indicative of the presence of small amounts of respective merocyanine isomers in the equilibrium (Scheme 3) with the predominant ring-closed forms. The ring-closed form is also prevalent for spiropyran **3** having a nitro group in the benzopyran ring. However, in this case the equilibrium amount of the merocyanine isomer increases to 1−2% in ethanol, which corresponds to the equilibrium constant $K_{296} = 1.6 \times 10^{-2}$. From the temperature dependence of the **3(Sp)** ⇄ **3(Mc)** equilibrium, its thermodynamic parameters have been determined: $\Delta G°_{296} = 10.2$ kJ·mol^{-1}, $\Delta H° = 2.9$ kJ·mol^{-1}, and $\Delta S° = -24.7$ J·mol^{-1}·K^{-1}. The absorption spectra of the ring-closed forms of compounds **1**−**4** are very slightly affected by solvents and the temperature of the solution. Table 1 contains the data on spectral properties of spiropyrans **1**−**4**.

UV irradiation of isopentane/2-propanol (4:1) solutions of spiropyrans **1**−**4** cooled to temperatures lower than 250 K results in the intense coloration caused by the photoinitiated ring-opening reaction resulting in the formation of the merocyanine isomers. Figure 1 pictures the spectral changes of the rearranged system, as exemplified by spiropyran **2**. The spectral pattern

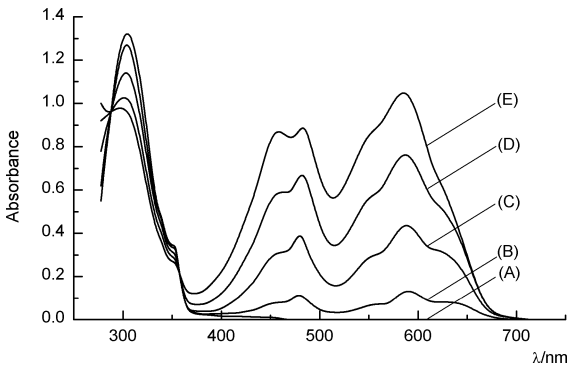

Figure 1. Absorption spectra of spiropyran **2** in the mixture isopentane/2-propanol (4:1) ($[C]_0 = 6.3 \times 10^{-5}$ mol·L^{-1}, $T = 77$ K) before (A) and after irradiation with 313 nm light for 60 (B), 180 (C), 360 (D), and 630 (E) s.

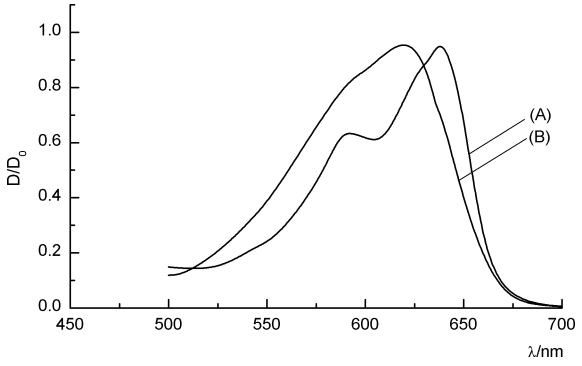

Figure 2. Normalized absorption spectra of spiropyran **3** in the mixture isopentane/2-propanol (4:1) ($[C]_0 = 5.6 \times 10^{-5}$ mol·L^{-1}, $T = 77$ K) after irradiation with 313 nm light for 300 (A) and 1200 (B) s.

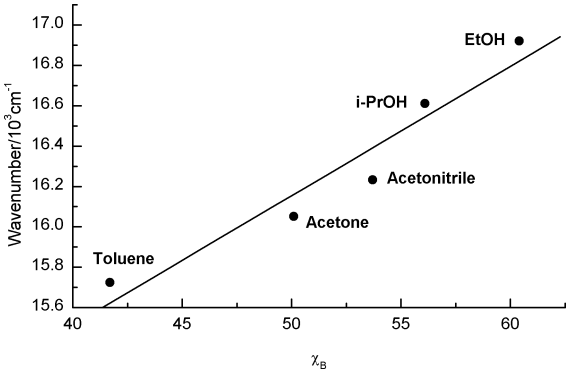

Figure 3. Linear relationship between the wavenumber $\nu_B = 1/\lambda_B$ of the absorption maximum of the colored forms of spiropyran **3** and the χ_B (blue shift) Brooker's solvatochromic parameters.[28]

closely resembles those reported for other photochromic spiropyrans rearranging according to the mechanism shown in Scheme 1.[1,2] The long wavelength absorption maxima of the merocyanines **1**−**4(Mc)** appearing at 585−592 and 482−483 nm (with, respectively, two and one shoulders) are assigned to $S_0 \rightarrow S_1$ and $S_0 \rightarrow S_2$ electronic transitions in the most stable, presumably **TTC**, merocyanine conformer. As seen from Figure 1, illumination of the solution of **2(Sp)** with the 313 nm light (with intensity 0.3×10^{16} quanta/s) results in the fast accumulation of the colored merocyanine isomer **2(Mc)**, whereas the formation of the intermediate **X** has not been traced under these conditions with the use of absorption and fluorescent spectra. No back **Mc** → **Sp** photoreaction occurs at 77 K. In general, the photoinitiated ring-opening reaction may result in the formation of not only **TTC** and **CTC** conformers shown in Scheme 3, but also of two additional conformers, **CTT** and **TTT**, with trans configuration at the central CC bond of a merocyanine.[3] Before reaching a photostationary state, the four conformers of the ring-opened merocyanine undergo photochemical and thermal rearrangements leading to equilibration, in which the most stable **TTC** and **CTC** forms are predominant.[3,27] Such a type of photoinduced equilibration reactions can be substantially slowed in viscous or rigid glassy media. We were able to trace the corresponding transformations by observing spectral changes occurring immediately after UV illumination of the solid isopentane/2-propanol solutions of spiropyrans **1**−**4** at 77 K. Thus, as shown in Figure 2, the absorption band with a maximum at 644 nm that appears immediately after UV illumination of the solution of spiropyran **3** under continuous illumination gradually shifts to 625 nm. Table 2 contains data on spectral properties of spiropyrans **1**−**4** in isopentane/2-propanol solutions before and after their UV illumination on reaching the photostationary states. For spiropyran **3**, it is possible to detect the absorption spectra of merocyanine **3(Mc)** formed upon irradiation of solutions of **3** in a series of solvents at room temperature. The positions of the absorption maxima have been found to be solvent sensitive (negative solvatochromism). The absorption frequencies well correlate with Brooker's χ_B solvatochromic parameters[28] (Figure 3). This correlation may be regarded (see ref 19) as an indication of the prevailing contribution of the zwitterionic forms to the resonance hybrid describing the structure of merocyanine **3(Mc)**. This conclusion is in agreement with the results of X-ray structural determinations[29] of a series of **TTC** conformers of merocyanine isomers of 6-nitro- and 8-nitro-1′,3′,3′-trimethylspiro[2*H*-1-benzopyran-2, 2′-indolines] that differed from **3** only by the absence in their molecules of a tetramethylenefuran fragment and also with the geometries and charge distributions calculated for **3** in various solvent environments. Results of the calculations carried out with the use of the Solvent Model 5.4/PM3 method intended to provide insight into the responses of a molecular structure to the effects of solvation are shown in Figure 4. It is seen that with increase in polarity of a solvent the double bond character of the central CC bond of **3** increases and those of the adjacent CC bonds decrease. The higher polarity of a solvent, the higher is the $N(CH_3) \rightarrow (C{=}O)$ and $N(CH_3) \rightarrow (NO_2)$ charge transfer along the chain of the conjugated bonds. Worth noting is that although the C═O bond of **3** in polar solvents is elongated compared with that in toluene, it does not approach the typical length of a phenolate CO bond. These data point to the zwitterionic structure of **3** to which the aci-nitro resonance structure **3(c)** bears a contribution. An appreciable contribution of such a resonance form has been recently indicated for the case of a close thione analogue of merocyanine **3**.[30] The spectral behavior of spiropyran **4** in isopentane/2-propanol solutions at temperatures higher than ∼100 K (Figure 5) is similar to that of **1**−**3**. The spectral changes portrayed by Figure 5 occur under irradiation of a solution of **4(Sp)** at 178 K with more intense light (2.9×10^{16} quanta/s), but are accompanied by a significantly slower accumulation of the colored **Mc** species than in the case of **2(Sp)**. The established photostationary equilibrium contains a low concentration of the **Mc** isomers. Such photo-

TABLE 2: Wavelengths of Maximum Absorption and Luminescence λ_{max} (in nm) of the Isomeric Forms of Spiropyrans 1−4 in Isopentane/2-Propanol Solutions at 77 K

compound	isomeric form	absorption	excitation of fluorescence	fluorescence	excitation of phosphorescence	phosphorescence
1	Sp	301, 346[a]			346	540, 585
	Mc	482, 546, 587, 627	470, 610	648, 695		
2	Sp	302, 348[a]	348	374	345	548, 577
	Mc	458, 482, 550,[a] 585, 625[a]	473, 550, 585, 626	659, 718		
3	Sp	298, 380[a]			382	512, 553, 598
	Mc	483, 592,[a] 625, 644[a]	468, 620	656, 710		
4	Sp	312, 379	379	540, 570[a]		
	X	471	468	543, 572		
	Mc	482, 550,[a] 585, 625[a]	480, 582, 625	653, 698[a]		

[a] A shoulder.

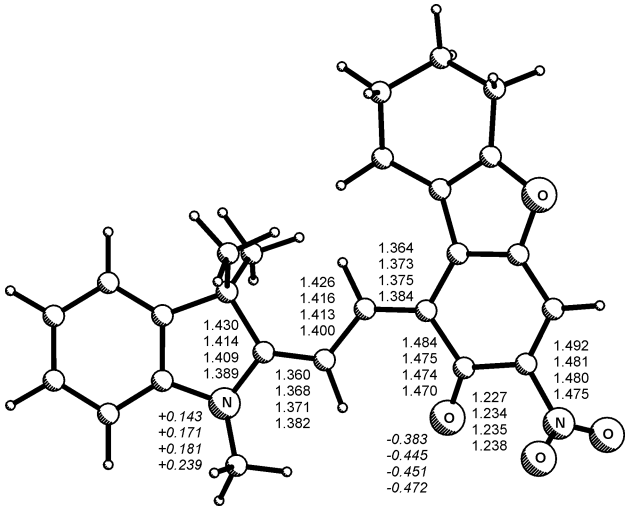

Figure 4. Bond lengths and electronic distributions (italics) in the **TTC** merocyanine isomer of spiropyran **3** calculated in various solvent environments using the SM5.4/PM3 method.[26a] The figures placed from the top to the bottom correspond to increase in the polarity of a solvent in the following order: toluene, ethanol, acetonitrile, dimethyl sulfoxide.

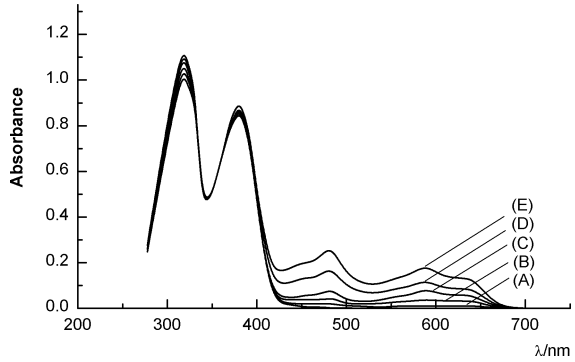

Figure 5. Absorption spectra of spiropyran **4** in the mixture isopentane/2-propanol (4:1) ($[C]_0 = 9.4 \times 10^{-5}$ mol·L^{-1}, $T = 178$ K) before (A) and after irradiation with 365 nm light for 600 (B), 1500 (C), 2700 (D), and 4800 (E) s.

chemical behavior cannot be a consequence of the dark back **Mc** → **Sp** reaction because this reaction does not proceed for spiropyrans **1**−**4** even at 250 K. However, at 77 K irradiation of an isopentane/2-propanol solution of **4** at 365 nm leads to the appearance of the longest wavelength absorption with a maximum at 471 nm (Figure 6). No formation of the corresponding **Mc** isomers has been observed under these conditions (spectral curves A−F). Irradiation of the solution in the region of the longest wavelength of **4(X)** induces the fast back **X** → **Sp** photoreaction. After establishing the photostationary equilibrium initiated by illumination with the light at 365 nm, further prolonged irradiation with nonfiltered light of a mercury lamp gives rise to the appearance of the 585−625 nm long wavelength absorption band (spectral curve G) manifesting the formation of the **4(Mc)** isomeric form. This is confirmed by the identity

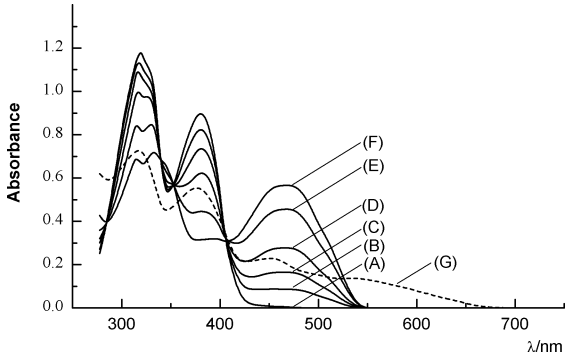

Figure 6. Absorption spectra of spiropyran **4** in the mixture isopentane/2-propanol (4:1) ($[C]_0 = 9.4 \times 10^{-5}$ mol·L^{-1}, $T = 77$ K) before (A) and after irradiation with the 365 nm light of a mercury lamp for 180 (B), 480 (C), 1080 (D), 4800 (E), and 9600 (F) s and after irradiadiation with the nonfiltered light of a mercury lamp for 1800 s (G).

of its fluorescent and excitation of fluorescence spectra with those characteristic of the **Mc** form obtained at 178 K. The dynamics of the spectral transformations occurring under irradiation is characterized by four isobestic points, which is indicative of the formation of a single species absorbing at $\lambda_{max} = 471$ nm and preceding the formation of the ultimate product of the photorearrangement. The observed spectral behavior may be explained as a consequence of the kinetic stabilization of the intermediate cis−cisoid isomer **4(X)** (Scheme 3, R = *t*-Bu), the bulky *tert*-butyl group of which creates a sufficiently high energy barrier to the rotation around the central CC bond and hinders the dark reaction in the rigid matrix at 77 K. This assignment is supported by the TD- B3LYP/6-31G** calculation of the absorption spectrum of **4(X)**. It is known that for conjugated molecules results of such a type of calculations are very sensitive to the input molecular geometries, in particular to the degree of bond length alternation, i.e., to the difference in length between the adjacent single and double bonds in the conjugated system, and to its deviation from planarity. On the basis of extensive calculations of absorption properties of various conjugated organic chromophores, it was concluded[31] that the TD-DFT computed spectral properties may be more accurately predicted when the input geometries obtained at the Hartree−Fock level of approximation are used since the DFT B3LYP approach tends to slightly overestimate electronic delocalization and, hence, equalization of the lengths in the conjugated chains. By the TD-B3LYP/6-31G**//RHF/6-31G** method, the positions of the two longest wavelength absorption maxima of the intermediate **4(X)** were calculated at 473 nm (2.62 eV, $f = 0.1618$) and 412 nm (3.01 eV, $f = 0.1552$), which is in good agreement with the experimental data (471 nm, 2.62 eV; the next absorption band is strongly overlapped with the near-lying others) for isopentane/2-propanol solution (Figure 6). At the same time, the TD-DFT//HF scheme cannot be applied to calculation of spectra of the merocyanine isomers due to the RHF → UHF instability and large spin contamination ($\langle S^2 \rangle = 2.04$) of the UHF solution caused by a contribution of the

SCHEME 4: Main Resonance Structures of the Merocyanine Form of 3

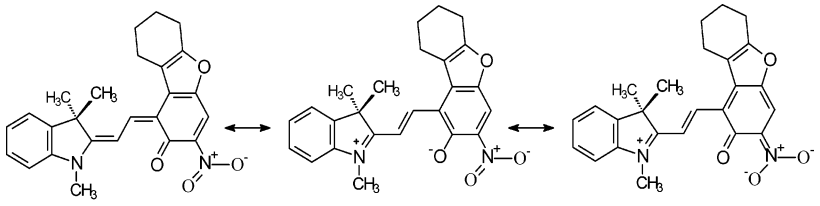

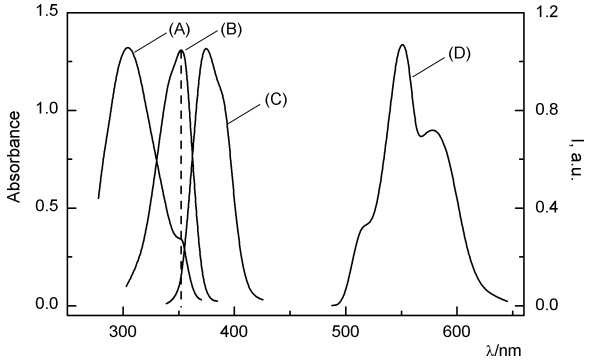

Figure 7. Absorption (A), excitation fluorescence (B), fluorescence (C), and phosphorescence (D) spectra of spiropyran **2** in the mixture isopentane/2-propanol (4:1) ($[C]_0 = 8.7 \times 10^{-5}$ mol·L^{-1}, $T = 77$ K).

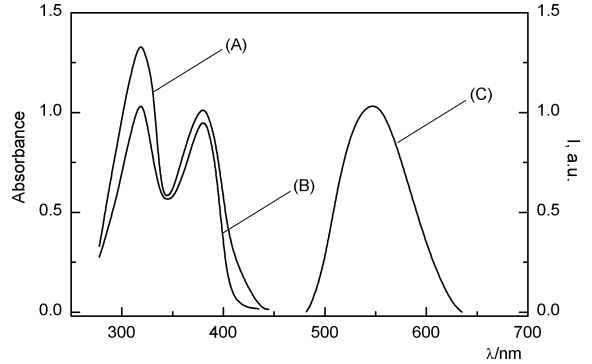

Figure 8. Absorption (A), excitation fluorescence (B), and fluorescence (C) spectra of spiropyran **4** in the mixture isopentane/2-propanol (4:1) ($[C]_0 = 9.3 \times 10^{-5}$ mol·L^{-1}, $T = 293$ K).

biradical component of the zwitterionic structure of **4(Mc)** forms. Spectrum of the nonconjugated ring-closed form **4(Sp)** was calculated by usual scheme TD-B3LYP/6-31G**//B3LYP/6-31G** to give the absorption maxima at 345 nm (3.52 eV, $f = 0.0808$) and 311 nm (3.99 eV, $f = 0.0560$), which can be compared with the experimental data (380 nm, 3.26 eV, and 312 nm, 3.97 eV, respectively). The difference between experimental and calculated transition energies within 0.2−0.3 eV is usually considered typical of the TD B3LYP approach.[32]

3.2. Luminescence Properties. The ring-closed forms of spiropyrans possess either very low intensity fluorescence or do not possess this property at all.[1,2,33] Among spiropyrans **1**−**3**, only **2** displays low intense fluorescence of the ring-closed form at 374 nm with a Stokes shift $\Delta\nu \cong 2000$ cm^{-1} in isopentane/2-propanol solution (Figure 7, Table 2). The phosphorescence observed for the ring-closed forms of spiropyrans **2** and **3** witnesses the existence of a triplet channel of deactivation of the excited state of these compounds characteristic of spiropyrans with nitro and heavy atom group substituents.[1−3,5,8] By contrast with **1**−**3**, the fluorescence of spiropyran **4** (Figure 8) is characterized by the anomalous Stokes shift (ASS) $\Delta\nu =$ 7200−8150 cm^{-1}, the magnitude of which increases with increase in solvent polarity, whereas the quantum yields of the fluorescence decrease as the polarity of the solvent increases (Table 3).

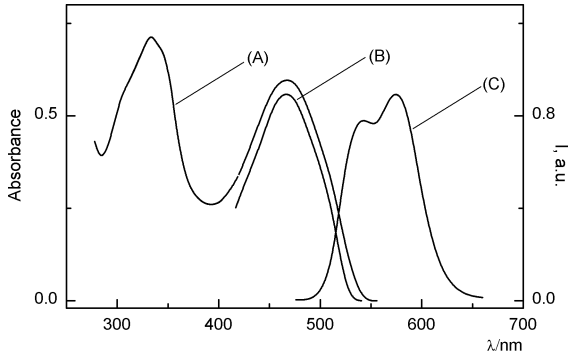

Figure 9. Absorption (A), excitation fluorescence (B), and fluorescence (C) spectra of spiropyran **4** preliminarily irradiated by the filtered (365 nm) light of a mercury lamp for 9600 s in the mixture isopentane/2-propanol (4:1) ($[C]_0 = 9.3 \times 10^{-5}$ mol·L^{-1}, $T = 77$ K).

Fluorescence spectra of the merocyanine isomers of spiropyrans **1**−**4(Mc)** contain low-intensity diffuse bands with maxima at 648−710 nm (Table 2). For **3(Mc)**, the quantum yield of fluorescence in ethanol solution is $\sim 10^{-3}$ ($\lambda_{max}^{flu} =$ 656 nm, $\lambda^{exc} =$ 468, 620 nm). The fluorescence of the intermediate photoproduct **4(X)** initially formed on irradiation of a rigid isopentane/2-propanol solution of **4(Sp)** at 77 K appears as the bands at 543 and 572 nm (Figure 9) in the same spectral region as the ASS fluorescence of the latter observed at room temperature. Prolonged irradiation at the longest wavelength of **4(X)** transforms its fluorescence spectrum to that characteristic of the merocyanine form **4(Mc)** with $\lambda_{max}^{flu} =$ 653 nm and a shoulder at 698 nm (Table 2). These results indicate that the origin of the ASS fluorescence of **4(Sp)** is associated with the fast rearrangement of its structure occurring in the S_1 electronic excited state due to the cleavage of the C_{spiro}−O bond and the formation of the cis−cisoid merocyanine intermediate **4(X)**. The CIS/3-21G** calculations performed have shown, indeed, that the S_1 PES of **4** contains a local minimum corresponding to such an intermediate (Figure 10), the structure of which is similar to that calculated for the cis−cisoid intermediate in its ground state (Figure 11). The excitation energies calculated by the CIS method are expectedly overestimated, but a recognized advantage of the method is that it well predicts changes in geometry occurring on the $S_0 \rightarrow S_1$ excitations and provides for correct characters of stationary points on the S_1 PES.[34] The appearance of the intermediate **4(X)** on the S_1 PES helps to explain the ASS of the fluorescence of **4**. Because of the steric hindrances produced by a bulky *tert*-butyl group in **4(X)**, the energy barrier against the rearrangement of **4(X)** to the merocyanine in the excited state is expected to be substantially increased compared with those for spiropyrans

TABLE 3: Fluorescent Properties of Solutions of Spiropyran 4 in Different Solvents at 293 K

	λ_{max}/nm			
solvent	absorption	excitation of fluorescence	fluorescence	quantum yield of fluorescence
hexane	312	316	515	0.012
	376	375		
toluene	318	320	526	0.008
	379	380		
ethanol	316	321	532	0.003
	378	378		
acetonitrile	316	318	542	0.003
	375	376		

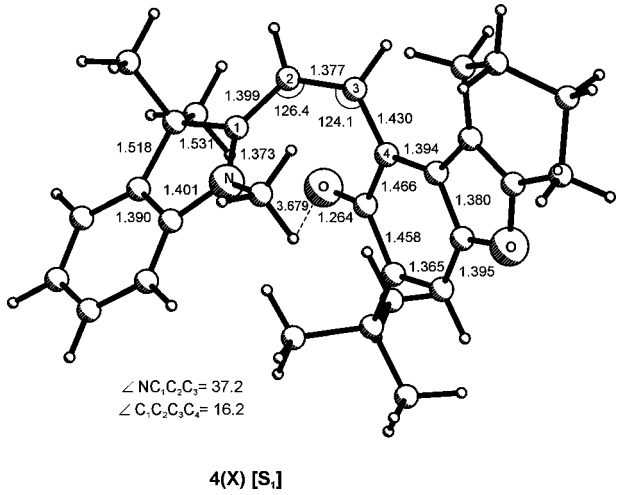

Figure 10. CIS/3-21G** computed geometry of intermediate **4(X)** on the S_1 PES. Bond lengths are in angstroms, and angles are in degrees.

1−**3**. This leads to extension of the lifetime of **4(X)** in the S_1 excited state, which allows detection of the fluorescence.

Therefore, on the basis of the data presented, the mechanism of the photoinitiated transformations of spiropyrans **1**−**4** can be described by the general Scheme 5.

3.3. Quantum Mechanical Modeling. This explanation is corroborated by the results of the DFT calculations of the detailed mechanism of the rearrangement of spiropyran **4** performed at B3LYP/3-21G** and B3LYP/6-31G** levels of approximations, the applicability of which to calculations of energy profiles of ground state reactions is well documented.[35]

SCHEME 5: General Scheme of Photoinitiated Transformations of Spiropyrans 1−4[a]

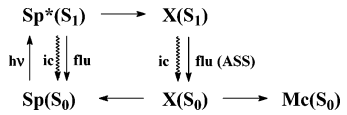

[a] ic, internal conversion; flu, fluorescence; flu(ASS), anomalous Stokes shift fluorescence.

By contrast with the properties of excited states, the above-mentioned drawback of the DFT method related to the slight overestimation of the bond length alterations (BLA) effect[31] has very little influence on the ground state energies.[35] Since all photochemical reactions begin and terminate on the ground state potential energy surface, we have first examined the minimal energy reaction path (MEP) for the thermal rearrangement of **4**. The structures of all transition states and intermediates appearing along the two possible MEPs leading from the ring-closed spirocyclic to the most stable (**TTC** and **CTC**) ring-opened merocyanine isomeric forms of **4** are depicted in Scheme 6 and Figures 11−14. The energy characteristics of these structures are listed in Table 4 and also shown in Figure 14, which portrays the energy profile of the **4(Sp)** ⇌ **4(Mc)** rearrangement. The bond lengths calculated for **4(Sp)** (Figure 11) are generally in good agreement (within the ±0.01−0.02 Å range) with the values obtained in X-ray determinations of spiropyrans **1**−**3(Sp)**.[16] A distinctive feature of the structure of **4(Sp)** is its significantly stretched C_{spiro}−O bond, the B3LYP/3-21G** calculated length of which is 0.045 Å longer than those X-ray determined[16] for **1(Sp)** and **1**−**2(Sp)**, respectively. As for **1**−**3(Sp)** and other spirobenzopyranindolines,[29] the pyran

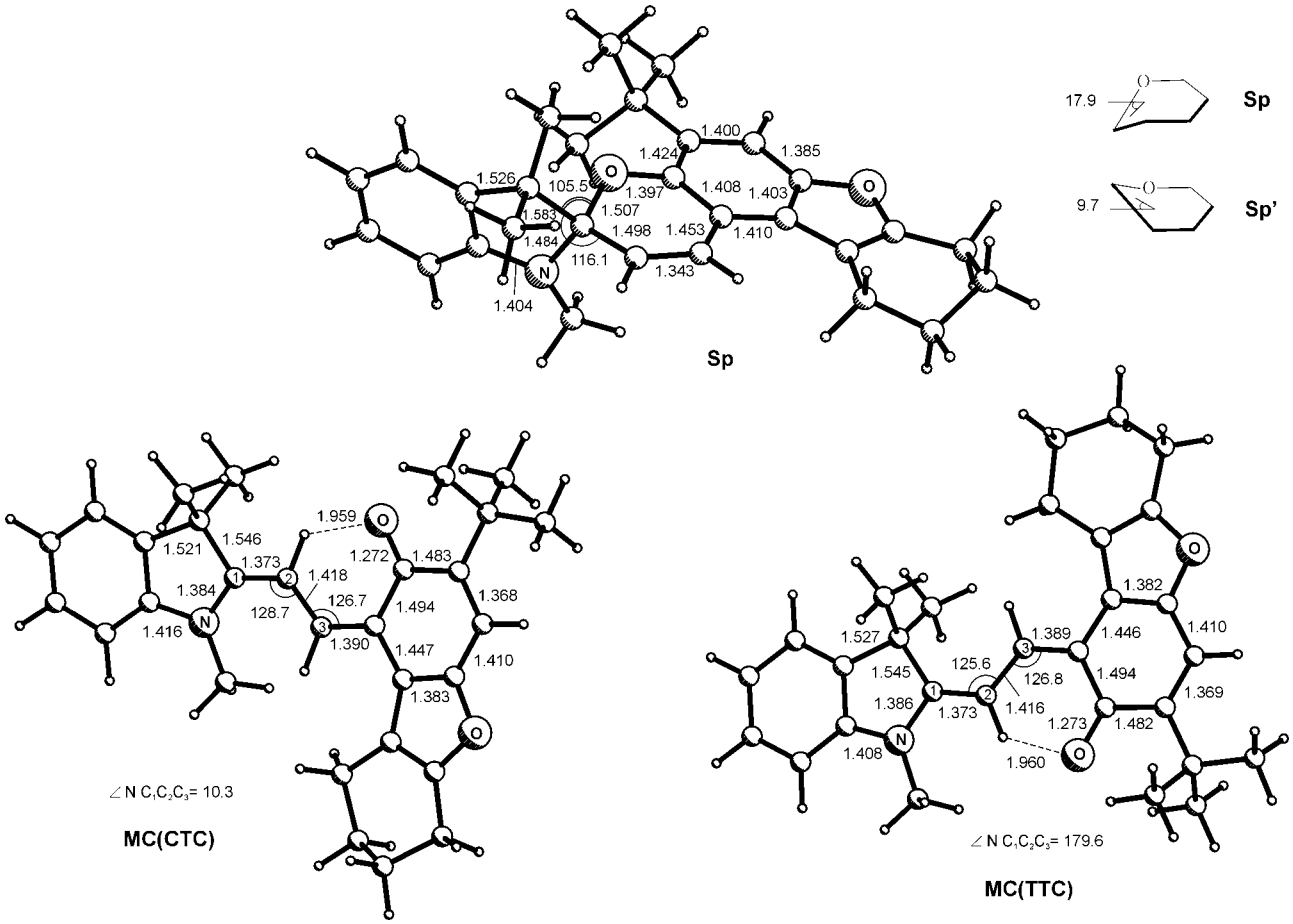

Figure 11. B3LYP/3-21G** computed geometries of the spirocyclic and merocyanine isomers of spiropyran **4**. Bond lengths are in angstroms, and angles are in degrees.

SCHEME 6: Minimal Energy Paths for Thermal Rearrangement of the Conformers of Spiropyran 4 (R = *tert*-Bu) as Calculated by the B3LYP/3-21G Method**

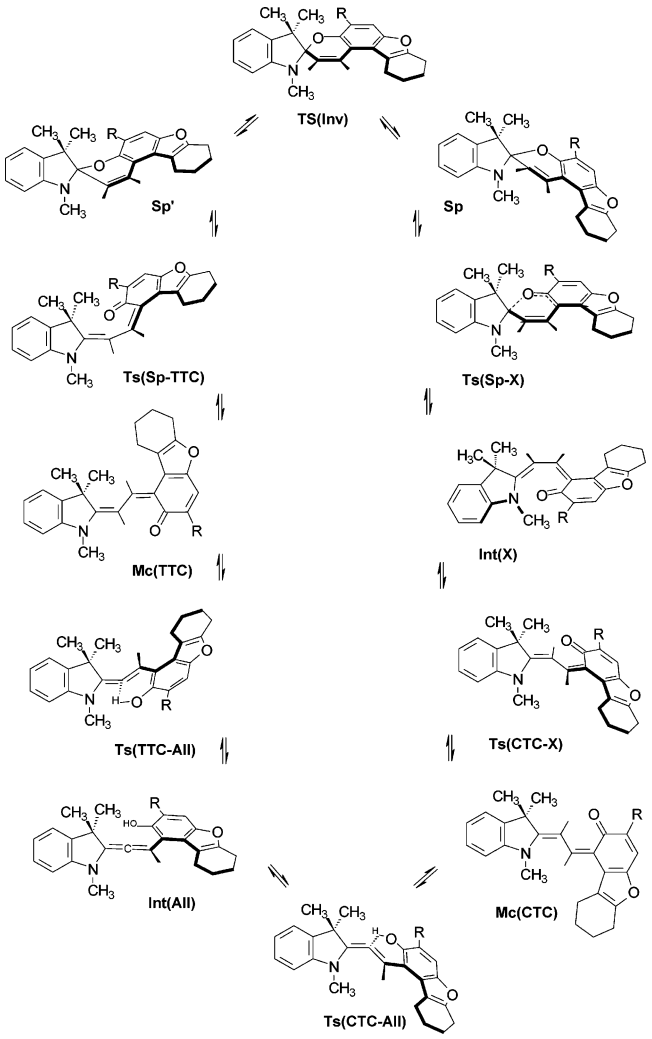

ring in **4(Sp)** is folded along the C(3)−O line. The calculations reveal two virtually energy equivalent and readily interconvertible (the calculated barrier is less than 2 kJ·mol^{-1}) conformers of the spirocyclic isomer of **4** shown in Scheme 6 as **Sp** and **Sp′** with bending along the C(3)−O line by 9.7° and 17.9°, respectively. It may be noted that in one X-ray study of 1′,3′,3′-trimethyl-6-nitrospiro[2*H*-1-benzopyran-2,2′-indoline], usually abbreviated as 6-NO_2-BIPS, similar conformers were found to exist in a crystal as independent molecules.[36] The calculated

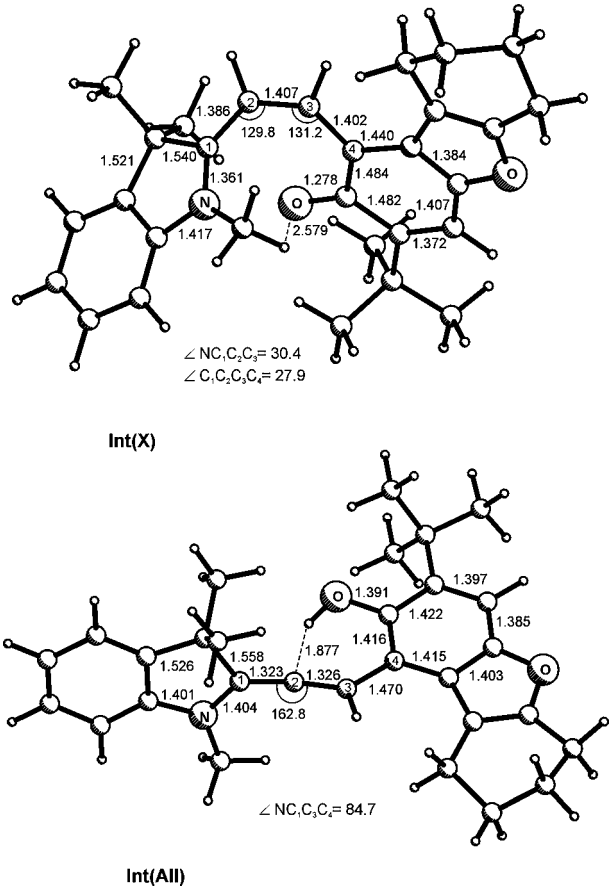

Figure 12. B3LYP/3-21G** computed geometries of the intermediates **Int(X)** and **Int(All)** occurring in the ring-opening reaction of spiropyran **4(Sp)**. Bond lengths are in angstroms, and angles are in degrees.

geometries of the merocyanine isomers of **4** (Figure 11) reveal the effects of equalization of the lengths of the conjugated CC bonds as well as the substantial elongation of the carbonyl CO bond, which features the substantial zwitterionic character of these structures. In accordance with the experimental data, the ring-closed spirocyclic isomer **Sp** is calculated to be the most stable isomeric form of **4**, which is 16.3 kJ·mol^{-1} energy favorable compared with its most stable ring-opened merocyanine form **Mc(TTC)**.

As seen from Scheme 6 and Figure 14, the rearrangement starts with stretching and cleavage of the C_{spiro}−O bond of **4(Sp)** and splits into the two distinguishable disrotatory-like reaction paths (since oxygen in the 2*H*-pyran ring has no substituents, the assignment to a particular mode of the rearrangement is arbitrary) starting from the conformers **Sp** and **Sp′**, respectively,

TABLE 4: Total Energies, Total Energies with Zero Point Energy (ZPE) Corrections, and Relative Energies of Structures Corresponding to the Stationary Points on the PES for the Thermal Isomerization of Spiropyran 4[a]

	B3LYP/3-21G**		B3LYP/6-31G**//B3LYP/3-21G**	
structure	E_{tot} + ZPE/au	ΔE/kJ·mol^{-1}	E_{tot}/au	ΔE/kJ·mol^{-1}
Sp	−1322.476 008	0	−1330.211 818	0
Sp	−1322.475 249	2.0	−1330.211 423	1.0
Ts(Sp-X)	−1322.449 195 (i171.8, 22.9)	70.3	−1330.187 510	64.0
Int(X)	−1322.450 903	66.1	−1330.193 259	48.5
Ts(CTC-X)	−1322.432 510 (i265.1, 15.2)	123.4	−1330.175 746	94.6
Mc(CTC)	−1322.458 438	47.7	−1330.201 966	25.9
Ts(CTC-All)	−1322.435 745 (i1282.2, 21.9)	105.9	−1330.170 953	107.1
Int(All)	−1322.444 681	82.4	−1330.183 526	74.5
Ts(TTC-All)	−1322.435 281 (i1300.7, 24.2)	107.1	−1330.170 878	107.5
Mc(TTC)	−1322.462 153	35.1	−1330.205 682	16.3
Ts(Sp-TTC)	−1322.432 536 (i235.8, 20.2)	114.4	−1330.177 085	91.2

[a] Imaginary and lowest real frequencies for the transition states are given in parentheses in cm^{-1}.

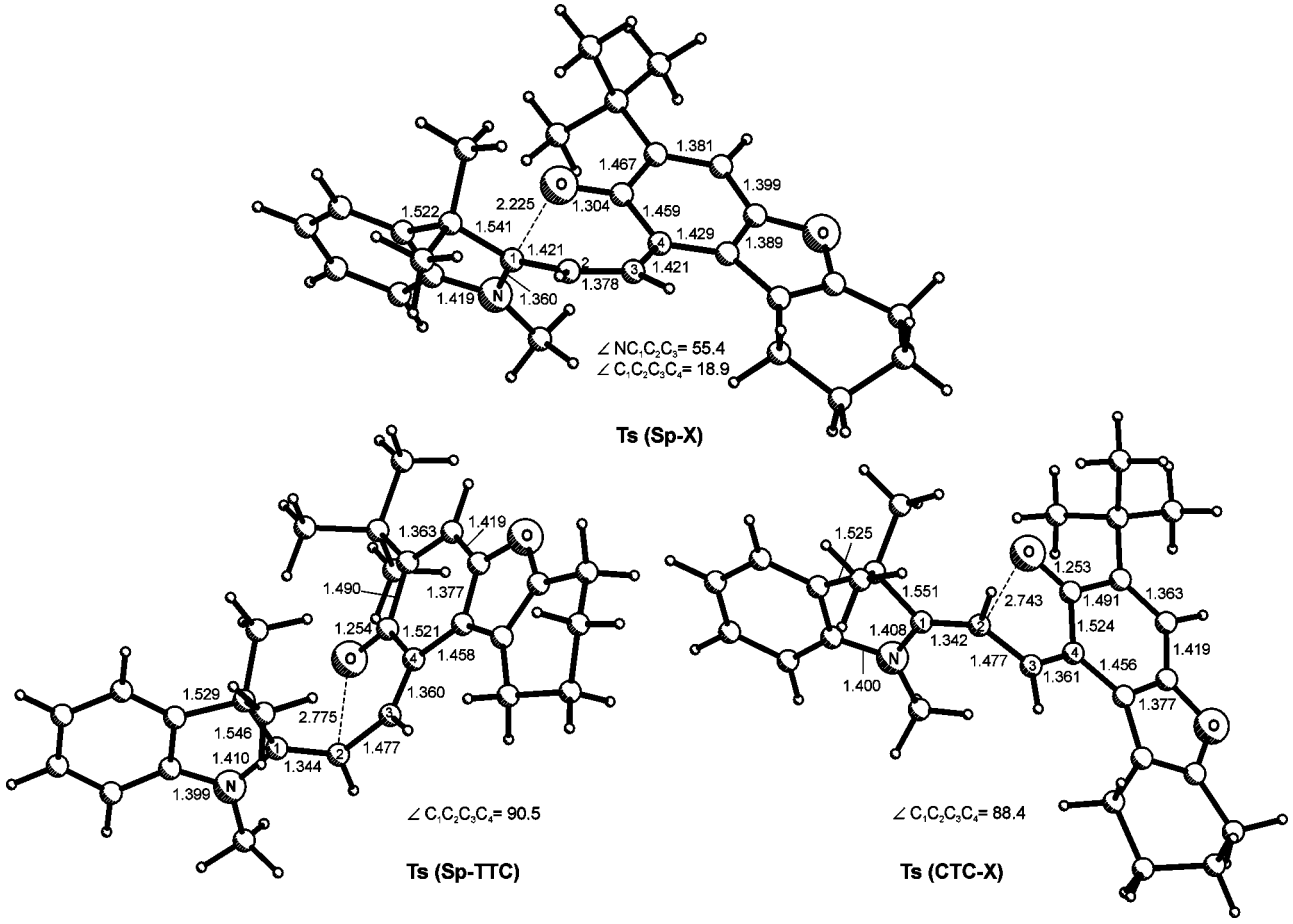

Figure 13. B3LYP/3-21G** computed geometries of the transition state structures **Ts(Sp-X)**, **Ts(Sp-TTC)**, and **Ts(CTC-X)** (Scheme 6). Bond lengths are in angstroms, and angles are in degrees.

to routes 1 and 2 in Figure 15. The branching of the MEP for the thermal interconversion of 2*H*-pyran and 2,4-pentadienal was also revealed by the previous semiempirical calculations of the mechanism of this electrocyclic reaction,[37] as well as the recent B3LYP/6-31G* calculations[38] of the mechanism of the conversion reactions of a model spirobenzopyranindoline derived from the archetypal 1′,3′,3′-trimethyl-6-nitrospiro[2*H*-1-benzopyran-2,2′-indoline] (6-NO_2-BIPS) through substitution of the geminal methyl groups at the tetrahedral 3′-carbon by hydrogen atoms. However, in those cases the bifurcation of the minimal energy paths (MEPs) originated from the existence on the PES of two energy close disrotatory- and conrotatory-like reaction valleys. For spiropyran **4**, one of these reaction channels (that for which the rotations about the CC bonds of the structure formed upon cleavage of the C_{spiro}−O bond result in drawing the geminal 3,3′-methyl and 6-*tert*-butyl groups closer together) is sterically blocked and the occurrence of two MEPs of the ring-opening reaction is due to the differences in the structure and vibrational spectra of the starting conformers.

When analyzing MEPs of the electrocyclic reactions, it is usually convenient to choose as the starting point a ring-opened structure,[39] the part of which is played in the **4(Sp)** ⇌ **4(Mc)** rearrangement by the most energy favorable merocyanine form **Mc(TTC)**. In a semiempirical (MNDO/PM3) study,[40] the mechanism of the merocyanine−spiropyran interconversion has been examined for the case of 6-NO_2-BIPS and interpreted as the stepwise transformation of the ring-opened isomer (of the **TTC** type) to the corresponding cis−cisoid (**CCC**) form occurring through sequential rotations about the CC bonds of the =C−CH−CH−C= triad. Our calculations showed that at the initial stages of the reaction paths of the rearrangement all the rotations are strongly coupled along the intrinsic reaction coordinates[41] (IRC). A similar conclusion has been also made on the basis of DFT calculations[42] of the mechanisms of the thermal cyclization reactions of spiroindolinenaphthoxazines, which are close structural analogues of spiropyranindolines. As seen from Figure 14, no local minima on the PES corresponding to intermediates of the ring-closing reaction were found when moving along route 2, which terminates in the **Sp′** conformation of **4(Sp)**. Much more complicated is the alternative reaction path (route 1), where the rotation about the central −CH−CH− bond of the **Mc(TTC)** form serves as the principal component of the reaction coordinate and the cyclization results in the formation of the **Sp** conformation of **4(Sp)** with the almost planar pyran ring. At the first stage of the multistep ring-opening reaction, stretching and cleavage of the C_{spiro}−O bond accompanied by the rotation about the =CH−CH= bond for ∼28° leads to the formation of the skewed cis−cisoid (**CCC**) intermediate denoted in Scheme 6 as **Int(X)** (Figure 12), which then rearranges to the merocyanine **Mc(CTC)**. A local minimum corresponding to the **CCC** structure has been also detected by the DFT calculations[38] of the MEPs of the thermal recyclization of 6-nitrospiro[2*H*-1-benzopyran-2,2′-indoline]. In the absence of the steric strain created by the geminal methyl groups at the 3′-carbon center, the cis−cisoid (**CCC**) conformer was found to be the most energy favored form among all possible merocyanine isomers of this model compound. The equilibrium between the **Mc(CTC)** and the most stable ring-opened isomer of the spiropyran, **Mc(TTC)**, is also established in two steps with the inclusion of the intermediate **Int(All)**. This allenic intermediate is formed through a low-energy barrier (58 kJ·mol^{-1}) 1,5-sigmatropic shift of a hydrogen atom along the

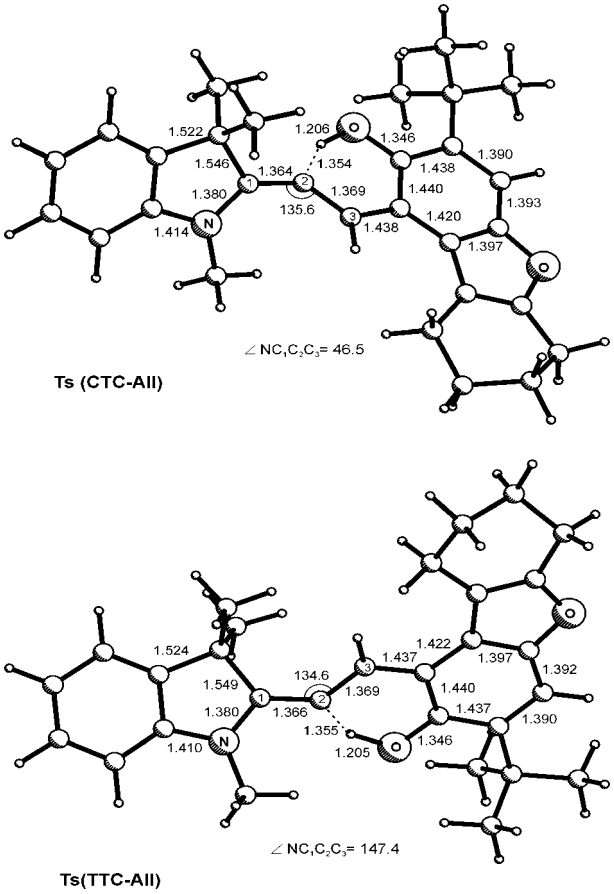

Figure 14. B3LYP/3-21G** computed geometries of the transition state structures **Ts(CTC-All)** and **Ts(TTC-All)** (Scheme 6). Bond lengths are in angstroms, and angles are in degrees.

C−H···O hydrogen bond of **Mc(CTC)**. As stems from the calculations (Figure 15, Table 4), its steady state concentration in the rearrangement depicted by Scheme 6 is expected to be negligible. However, intermediate species of such a type may play a more important role in the photochemical and thermal rearrangements of other spiropyrans and their structural analogues. Thus, the NMR monitoring of the photochromic rearrangement of 2,2-di(4-fluorophenyl)-6-methoxy-(2*H*-1)-chromene presented definite evidence for the involvement of a similar type *o*-allenyl-*p*-methoxyphenyl intermediate in the mechanism of the ring-opening reaction.[43] No such type of structures has yet been found in previous theoretical DFT and ab initio studies of the mechanisms of the electrocyclic reactions of spiropyrans and spirooxazines.[38,43,44]

The calculated geometries of the intermediates **Int(CCC)** and **Int(All)** are shown in Figure 12, and those for the transition state structures appearing along the "conrotatory" and "disrotatory" reaction paths of the ring-opening reaction are presented by Figures 13 and 14. In the B3LYP/6-31G**//B3LYP/3-21G** approximation, the energy barrier against the thermal ring-opening reaction of **4(Sp)** is estimated as 94.6 kJ·mol^{-1}, the value of which is close to that found for the activation energy barrier to the thermal ring-opening (coloration) reaction of spiropyran **3(Sp)** in ethanol solution, as discussed in the following section.

3.4. Kinetics of Photointiated and Thermal Rearrangements. The photocoloration of solutions of spiropyrans **1**−**4** was observed in a wide temperature interval of 77−296 K. The quantum yields of the direct and back photorearrangement reactions measured for **3** in ethanol at 285 K are 0.046 and 0.035, respectively. The molar absorption coefficient of the colored form at the maxima of the long wavelength absorption band is 54 300 L mol^{-1} cm^{-1}. For spiropyrans **1**−**3**, the rate of the back photoreaction significantly decreases with lowering the temperature of solution and at 77 K drops to zero. At 77 K the photobleaching reactions are fully retarded, which points to the existence of a substantial energy barrier to the ring closing of the **CTC** and/or **TTC** merocyanine isomeric forms (**Mc**) at

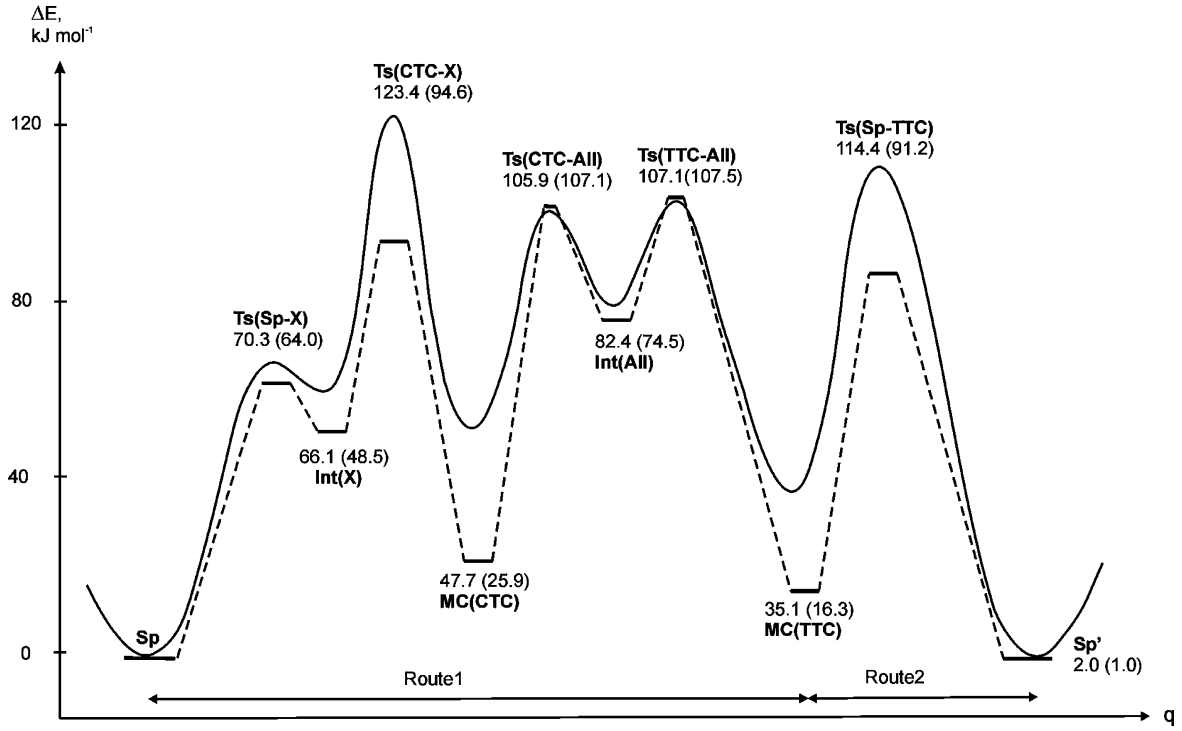

Figure 15. B3LYP/3-21G** ground state adiabatic potential energy profile for the reaction paths of the ring-opening/closing rearrangement of **4**. B3LYP/6-31G**//B3LYP/3-21G** energy levels calculated for the optimized structures corresponding to the local minima and saddle points are shown as the bold horizontal bars (relative energies in parentheses). Relative energies are in kilojoules per mole.

the S_1 electronic excited state. In the case of **4**, UV irradiation of its isopentane/2-propanol solution at 77 K gives rise to the intermediate **4(X)**. Continuing the irradiation brings about the subsequent photobleaching process: **4(X)** → **4(Sp)**. Kinetics of the back ring-closing reaction of spiropyrans is usually studied as the relaxation kinetics of merocyanine forms induced upon irradiation of a solution of the spirocyclic isomers.[45] For spiropyrans **1**, **2**, and **4**, these relaxation reactions are very fast at room temperature, which makes qualitative kinetic description of their kinetics difficult. An exception to this trend is the spiropyran **3**. The relaxation kinetics of **3(Mc)** → **3(Sp)** in ethanol is described by a monoexponential function. The following kinetic and activation parameters were obtained using the photokinetic modeling: $k_2(296\ \mathrm{K}) = 1.5 \times 10^{-2}\ \mathrm{s}^{-1}$; $E_a = 103.8\ \mathrm{kJ{\cdot}mol^{-1}}$. The thermal coloration process **3(Sp)** → **3(Mc)**, the kinetics of which was assessed using the same approach, is notably slower: $k_1(296\ \mathrm{K}) = 2.4 \times 10^{-4}\ \mathrm{s}^{-1}$; $E_a = 107.6\ \mathrm{kJ{\cdot}mol^{-1}}$.

4. Conclusion

The formation of a long-lived intermediate (**X**) on the reaction pathway of the photochromic rearrangement of 6-alkyl-1′,3′,3′-trimethyl-1,2-tetramethylenespiro[7*H*-furo(3,2-*f*)-(2*H*-1)-benzopyran-7,2′-indolines] **1**−**4** occurring under continuous UV irradiation of rigid isopentane/2-propanol solution at 77 K has been proved for the case of the *tert*-butyl derivative (R = *tert*-butyl) based on the measurements of the absorption and emission spectra and corroborated by the results of quantum mechanical calculations of the structure and spectral properties of the acoplanar cis−cisoid (**CCC**) intermediate **4(X)**. The appearance of the intermediate **4(X)** preceding the formation of the final products of the photoinitiated ring-opening reaction of spiropyrans **1**−**4(Sp)** explains the observed ASS fluorescence of **4(Sp)** (R = *tert*-butyl). The photocoloration of solutions of spiropyrans **1**−**4(Sp)** occurs at a wide temperature range of 77−293 K. The efficiency of the photobleaching processes decreases with lowering the temperature of solution.

Acknowledgment. This work was supported by the International Scientific Technological Center (Project No. 2117), the program Basic Research and Higher Education (REC-004), and the Ministry of Industry and Science of Russian Federation (Grant 945.2003.03).

Supporting Information Available: NMR spectral parameters of compounds **1**−**4**, data on photokinetic modeling of the rearrangements, B3LYP/3-21G**-optimized Cartesian coordinates of the stationary points, and CIS/3-21G**-calculated energy of the intermediate **4(X)** [S_1]. This material is available free of charge via the Internet at http://pubs.acs.org.

References and Notes

(1) (a) Guglielmetti, R. In *Photochromism: Molecules and Systems*; Dürr, H., Bouas-Laurent, H., Eds.; Elsevier: Amsterdam, 1990; p 314. (b) Bertelson, R. C. In *Organic Photochromic and Thermochromic Compounds*; Crano, J. C., Guglielmetti, R. J., Eds.; Topics in Applied Chemistry 1; Plenum Press: New York, 1999; p 11.

(2) (a) Berkovic, G.; Krongauz, V.; Weiss, V. *Chem. Rev.* **2000**, *100*, 1741. (b) Kawata, S.; Kawata, Y. *Chem. Rev.* **2000**, *100*, 1777.

(3) Minkin, V. I. *Chem. Rev.* **2004**, *104*, 2751.

(4) (a) Aramaki, S.; Atkinson, G. H. *J. Am. Chem. Soc.* **1992**, *114*, 438. (b) Yuzawa, T.; Takahashi, H. *Mol. Cryst. Liq. Cryst.* **1994**, *246*, 279.

(5) (a) Ernsting, N. P.; Arthen-Engel, T. *J. Phys. Chem.* **1991**, *95*, 5502. (b) Görner, H. *Chem. Phys. Lett.* **1998**, *282*, 381. (c) Rini, M.; Holm, A.-K.; Nibbering, E. T. J.; Fidder, H. J. *Am. Chem. Soc.* **2003**, *125*, 3028.

(6) Sakuragi, M.; Aoki, K.; Tamaki, T.; Ichimura, K. *Bull. Chem. Soc. Jpn.* **1990**, *63*, 74.

(7) (a) Malkin, Y. N.; Krasieva, T. B.; Kuzmin, V. A. *J. Photochem. Photobiol. A: Chem.* **1989**, *49*, 75. (b) Salemi, C.; Giusti, G.; Guglielmetti, R. *J. Photochem. Photobiol. A: Chem.* **1995**, *86*, 261.

(8) Chibisov, A. K.; Görner, H. *Phys. Chem. Chem. Phys.* **2001**, *3*, 424.

(9) Celani, P.; Bernardi, P. F.; Olivucci, M.; Robb, M. A. *J. Am. Chem. Soc.* **1997**, *119*, 10815.

(10) Heligman-Rim, R.; Hirshberg, Y.; Fischer, E. *J. Phys. Chem.* **1962**, *66*, 2470.

(11) (a) Krysanov, S. A.; Alfimov, M. V. *Chem. Phys. Lett.* **1982**, *91*, 77. (b) Antipin, S. A.; Petrukhin, A. N.; Gostev, F. E.; Marevtsev, V. S.; Titov, A. A.; Barachevsky, V. A.; Strokach, Y. P.; Sarkisov, O. M. *Chem. Phys. Lett.* **2000**, *331*, 378. (c) Zhang, J. Z.; Schwartz, B. J.; King, J. C.; Harris, C. B. *J. Am. Chem. Soc.* **1992**, *114*, 10921.

(12) Lokshin, V.; Samat, A.; Metelitsa, A. V. *Russ. Chem. Rev.* **2002**, *71*, 893.

(13) (a) Tamai, N.; Masuhara, H. *Chem. Phys. Lett.* **1992**, *191*, 189. (b) Tamai, N.; Masuhara, H. *Chem. Rev.* **2000**, *100*, 1875.

(14) (a) Pozzo, J.-L.; Samat, A.; Guglielmetti, R.; Lokshin, V.; Minkin, V. *Can. J. Chem.* **1996**, *74*, 1649. (b) Lukyanov, B. S.; Shepelenko, E. N.; Bren, V. A.; Bulanov, A. O. *Khim. Geterotsikl. Soedin.* **2000**, 987.

(15) (a) Rybalkin, V. P.; Bushkov, A. Ya.; Bren, V. A.; Minkin, V. I. *Zh. Org. Khim.* **1986**, *22*, 565. (b) Rybalkin, V. P.; Shepelenko, E. N.; Popova, L. L.; Dubonosov, A. D.; Bren, V. A.; Minkin, V. I. *Zh. Org. Khim.* **1996**, *31*, 101. (c) Rybalkin, V. P.; Dubonosov, A. D.; Shepelenko, E. N.; Popova, L. L.; Makarova, N. I.; Bren, V. A.; Tsukanov, A. V.; Minkin, V. I. *Zh. Org. Khim.* **2002**, *38*, 1381.

(16) Lukyanov, B. S.; Utenyushev, A. N.; Shepelenko, E. N.; Tkachev, V. V.; Lukyanova, M. B.; Metelitsa, A. V.; Besugliy, S. O.; Aldoshin, S. M.; Minkin, V. I. *Khim. Geterotsikl. Soedin.* **2005**, in press.

(17) Pimienta, V.; Frouté, C.; Deniel, M. H.; Lavabre, D.; Guglielmetti, R.; Micheau, J.-C. *J. Photochem. Photobiol. A: Chem.* **1999**, *122*, 199−204.

(18) Deniel, M. H.; Lavabre, D.; Micheau, J. C. In *Organic Photochromic and Thermochromic Compounds*; Crano, J. C., Guglielmetti, R. J., Eds.; Topics in Applied Chemistry 2; Plenum Press: New York, 1999; p 167.

(19) Metelitsa, A. V.; Lokshin, V.; Micheau, J. C.; Samat, A.; Guglielmetti, R.; Minkin, V. I. *Phys. Chem. Chem. Phys.* **2002**, *4*, 4340.

(20) Borderie, B.; Lavabre, D.; Micheau, J. C.; Laplante, J. P. *J. Phys. Chem.* **1992**, *96*, 2953−61.

(21) (a) Becke, A. D. *Phys. Rev. A* **1991**, *91*, 651. (b) Becke, A. D. *J. Chem. Phys.* **1993**, *98*, 5648.

(22) Lee, C.; Yang, W.; Parr, R. G. *Phys. Rev. B* **1988**, *37*, 785.

(23) Gross, E. K. U.; Kohn, W. *Adv. Quantum Chem.* **1990**, *21*, 255.

(24) Frisch, M. J.; Trucks, G. W.; Schlegel, H. B.; Scuseria, G. E.; Robb, M. A.; Cheeseman, J. R.; Zakrzewski, V. G.; Montgomery, J. A., Jr.; Stratmann, R. E.; Burant, J. C.; Dapprich, S.; Millam, J. M.; Daniels, A. D.; Kudin, K. N.; Strain, M. C.; Farkas, O.; Tomasi, J.; Barone, V.; Cossi, M.; Cammi, R.; Mennucci, B.; Pomelli, C.; Adamo, C.; Clifford, S.; Ochterski, J.; Petersson, G. A.; Ayala, P. Y.; Cui, Q.; Morokuma, K.; Malick, D. K.; Rabuck, A. D.; Raghavachari, K.; Foresman, J. B.; Cioslowski, J.; Ortiz, J. V.; Baboul, A. G.; Stefanov, B. B.; Liu, G.; Liashenko, A.; Piskorz, P.; Komaromi, I.; Gomperts, R.; Martin, R. L.; Fox, D. J.; Keith, T.; Al-Laham, M. A.; Peng, C. Y.; Nanayakkara, A.; Challacombe, M.; Gill, P. M. W.; Johnson, B.; Chen, W.; Wong, M. W.; Andres, J. L.; Gonzalez, C.; Head-Gordon, M.; Replogle, E. S.; Pople, J. A. *Gaussian 98*, revision A.9; Gaussian, Inc.: Pittsburgh, PA, 1998.

(25) GAMESS, version 12 Dec 2003 (R2). Schmidt, M. W.; Baldridge, K. K.; Boatz, J. A.; Elbert, S. T.; Gordon, M. S.; Jensen, J. H.; Koseki, S.; Matsunaga, N.; Nguyen, K. A.; Su, S. J.; Windus, T. L.; Dupius, M.; Montgomery, J. A. *J. Comput. Chem.* **1993**, *14*, 1347−1363.

(26) (a) Chambers, C. C.; Giesen, D. J.; Gu, M. Z.; Cramer, C. J.; Truhlar, D. G. *J. Phys. Chem.* **1997**, *101*, 2061. (b) Hawkins, G. D.; Giesen, D. J.; Lynch, G. C.; Chambers, C. C.; Rossi, I.; Storer, J. W.; Li, J.; Zhu, T.; Winget, P.; Rinaldi, D.; Liotard, D. A.; Cramer, Ch. J.; Truhlar, D. G. AMSOL, version 6.6.

(27) (a) Nakamura, S.; Uchida, K.; Murakami, A.; Irie, M. *J. Org. Chem.* **1993**, *58*, 5543. (b) Delbaere, S.; Bochu, C.; Azaroual, N.; Buntinx, G.; Vermeersch, G. *J. Chem. Soc., Perkin Trans. 2* **1997**, 1499.

(28) Brooker, L. G. S.; Craig, A. C.; Heseltine, D. W.; Jenkins, P. W.; Lincoln, L. L. *J. Am. Chem. Soc.* **1965**, *87*, 2443.

(29) Aldoshin, S. In *Organic Photochromic and Thermochromic Compounds*; Crano, J. C., Guglielmetti, R. J., Eds.; Topics in Applied Chemistry 2; Plenum Press: New York, 1999; p 297.

(30) Hirano, M.; Osakada, K.; Nohira, H.; Miyashita, A. *J. Org. Chem.* **2002**, *67*, 533.

(31) Masunov, A.; Tretiak, S. *J. Phys. Chem.* **2004**, *108*, 899.

(32) Guillaumont, D.; Nakamura, S. *Dyes Pigm.* **2000**, *46*, 85−92.

(33) Kuz'min, M. G. In *Organic Photochromes*; El'tsov, A. V., Ed.; Consultant Bureau: New York, 1990; p 246.

(34) (a) Foresman, J. B.; Head-Gordon, M.; Pople, J. A.; Frisch, M. J. *J. Phys. Chem.* **1992**, *96*, 135. (b) Orlova, G. A.; Goddard, J. D.; Brovko, L. Yu. *J. Am. Chem. Soc.* **2003**, *125*, 6962.

(35) (a) Ziegler, T. *Chem. Rev.* **1991**, *91*, 651. (b) Te Velde, G.; Bickelhaupt, F. M.; Baerends, E. J.; Fonseca Guerra, C.; van Gisbergen, S. J. A.; Snijders, J. G.; Ziegler, T. *J. Comput. Chem.* **2001**, *22*, 931.

(36) Karaev, S.; Furmanova, N. G.; Belov, N. V. *Dokl. Akad Nauk SSSR, Ser. Khim.* **1982**, *262*, 877.

(37) Pichko, V. A.; Simkin, B. Ya.; Minkin, V. I. *J. Org. Chem.* **1992**, *57*, 7087.

(38) Sheng, Y.; Leszynski, J.; Garcia, A. A.; Rosario, R.; Gust, D.; Springer, J. *J. Phys. Chem. B* **2004**, *108*, 16233.

(39) Houk, K. N.; Li, Y.; Evanseck, J. D. *Angew. Chem., Int. Ed. Engl.* **1992**, *31*, 682.

(40) Wojtyk, J. T.; Wasey, A.; Kazmayer, P. M.; Hoz, S.; Buncel, E. *J. Phys. Chem. A* **2000**, *104*, 9046.

(41) Fukui, K. *Acc. Chem. Res.* **1981**, *14*, 363.

(42) (a) Maurel, F.; Aubard, J.; Rajzmann, M.; Guglielmetti, R.; Samat, A. *J. Chem. Soc., Perkin Trans 2* **2002**, 1307. (b) Horii, T.; Abe, Y.; Nakao, R. *J. Photochem. Photobiol. A: Chem.* **2001**, *144*, 119.

(43) (a) Delbaere, S.; Micheau, J.-C.; Vermeersch, G. *Org. Lett.* **2002**, *4*, 3143. (b) Delbaere, S.; Micheau, J. C.; Vermeersch, G. *J. Org. Chem.* **2003**, *68*, 8968.

(44) (a) Day, P. N.; Wang, Z.; Patchter, R. *J. Phys. Chem.* **1995**, *99*, 9730. (b) Cottone, G.; Noto, R.; La Manna, G. *Chem. Phys. Lett.* **2004**, *388*, 218.

(45) (a) Kellmann, A.; Tfibel, F.; Dubest, R.; Levoir, P.; Aubard, J.; Pottier, E.; Guglielmetti, R. J. *Photochem. Photobiol. A* **1989**, *49*, 63. (b) Chibisov, A. K.; Görner, H. J. *J. Phys. Chem. A* **1999**, *103*, 5211.